THE BELL SYSTEM
TECHNICAL JOURNAL

DEVOTED TO THE SCIENTIFIC AND ENGINEERING
ASPECTS OF ELECTRICAL COMMUNICATION

Volume 51 March 1972 Number 3

Power Coupling from GaAs Injection Lasers into Optical Fibers

By L. G. COHEN

(Manuscript received October 4, 1971)

Measurements have been made to determine the efficiency of coupling light from GaAs injection lasers (λ = 9000 Å) of stripe geometry into the cores of optical fibers. Laser light was coupled into a fiber across a small air gap which separated the laser from the fiber. The power coupling efficiency was calculated by extrapolating the lasing light power emitted at the end of a short length of fiber back to its input tip and comparing it with the total laser beam power. Experiments were performed with several diffused junction (DJ) lasers and with low-threshold double-heterostructure (DH) lasers having stripes formed by proton bombardment or oxide masking. The beam profile, scanned in its near and far field region, was approximately Gaussian. The beam dimensions at the surface of the laser were estimated from far field measurements and were used to predict the coupling efficiency of single-mode and multimode fibers. Power coupling efficiencies of about 70 percent were measured for DJ lasers feeding 10-μm multimode fibers. A coupling efficiency of 25 percent, almost identical to the theoretical estimate, was achieved with a DH laser having a 1-μm × 13-μm proton-bombarded stripe, feeding the 3.2-μm core of a single-mode fiber. The coupling efficiency was greater than 40 percent when a DJ laser fed the same fiber. A cylindrical lens is proposed to increase the power coupling perpendicular to the junction plane.

Permanent self-supporting couplers were made by applying epoxy between structures which supported the fiber and the laser.

I. INTRODUCTION

This paper describes experiments performed to determine the efficiency of coupling light power from GaAs injection lasers* ($\lambda \approx 9000$ Å) into the cores of 3.2-μm and 3.7-μm single-mode fibers and several sizes of multimode fibers.† At one end of a fiber the light from a laser was coupled in across a small air gap which separated the laser from the fiber. The power coupling efficiency was computed by extrapolating the lasing light power emitted from a 30-cm length of fiber back to its input tip and comparing it with the total laser power. Permanent coupling of injection lasers and fibers was accomplished by applying epoxy between structures which supported the fiber and the GaAs chip. One other coupling technique was tried. It involved bonding (with epoxy) a fiber onto one of the laser mirrors. However, this technique was abandoned because application of epoxy to the active stripe on a GaAs chip raised the lasing threshold by 30 percent. Only 30 percent of this rise was attributable to the decrease in mirror reflectivity at the epoxy interface. The remaining discrepancy may have been caused by strains introduced to the mirror as the epoxy hardened.

The body of this paper is divided into three sections. In Section 2.1 we describe measurements to determine the properties of light beams emanating from double-heterostructure (DH) lasers and also from diffused junction (DJ) lasers of striped geometry. Guiding stripes on DH lasers were formed by oxide masking or proton bombardment. In proton-bombarded DH lasers the current is confined within a stripe by high-resistivity regions produced by proton bombardment at the edges of the stripe. The details of the fabrication and performance of proton-bombarded lasers are discussed in Ref. 1. Section 2.2 describes power coupling measurements for lasers feeding single-mode and multimode fibers. In Section III we propose a technique to increase the power coupling efficiency by attaching a cylindrical lens onto the fiber tip. The lens was designed to collimate the laser beam perpendicular to the junction plane in order to transform its cross section from a rectangular to a square shape. Finally, in Section IV we indicate how theoretical estimates of power coupling efficiency were made based on the measured properties of the laser beam.

---

* The lasers were fabricated by J. C. Dyment at Bell Laboratories, Murray Hill, N. J.

† The 3.7-μm fiber was fabricated by Corning Glass Works of Corning, N. Y. All the other fibers were drawn from glass preforms by DeBell and Richardson, Inc., of Hazardville, Conn.

II. MEASUREMENTS

Experiments have been performed to determine the efficiency for coupling light ($\lambda \approx 9000$ Å) into optical fibers from the radiation field of GaAs injection lasers. Laser light emanated from a rectangular aperture on the cleaved surface of the GaAs chip. The beam dimensions were about 3 μm $\times$ 6 μm for DJ lasers and about 1 μm $\times$ 3 μm for DH lasers. The GaAs laser chip was held, by spring contact, with its p-side face down on a copper block and was driven at room temperature at a 100-Hz repetition rate by negative current pulses, 100 nanoseconds wide, which were applied between the spring and the grounded copper block. Peak power measurements were displayed on a storage sampling oscilloscope.

2.1 *Laser Field Measurements*

The properties of the light beam emanating from the lasing aperature were determined by scanning its near and far field radiation patterns.

Far field measurements were made by rotating a laser about one of its cleaved surfaces in the plane parallel to the laser's junction plane and also in the plane perpendicular to it. The power distribution in the beam was measured as a function of angle, 1.5 inches from the laser, through a 10-mil slit mounted on a photomultiplier (refer to Fig. 1). The shape of the profiles was independent of the slit width and the axial separation between laser and slit.

Near field measurements[2] were made by using a lens to magnify the light pattern on the laser mirror. Magnification of X140 was obtained when a X40 microscope objective lens was used to focus the light pattern on a photomultiplier displaced 75 cm from the laser. This blown-up image was scanned through a 0.5-mil slit, attached to

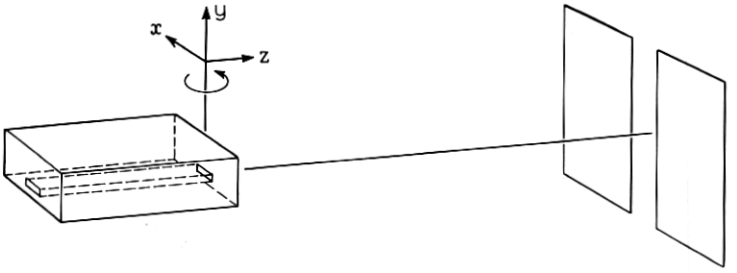

Fig. 1—Experimental arrangement to measure radiation profiles in the far field of a laser beam. The laser was rotated about one of its mirrors and the light power transmitted through a 10-mil slit was measured as a function of rotation angle.

the photomultiplier and aligned parallel or perpendicular to the junction plane.

Sample far field patterns are illustrated in Fig. 2 for a diffused junction laser, and also for two double-heterostructure lasers, one with an oxide-masked stripe and the other with a proton-bombarded stripe. Along the junction plane (Fig. 2a) the pattern of the DJ laser is more Gaussian-like than either of those for the DH lasers. The profile corresponding to the DH laser with the oxide-masked stripe has two

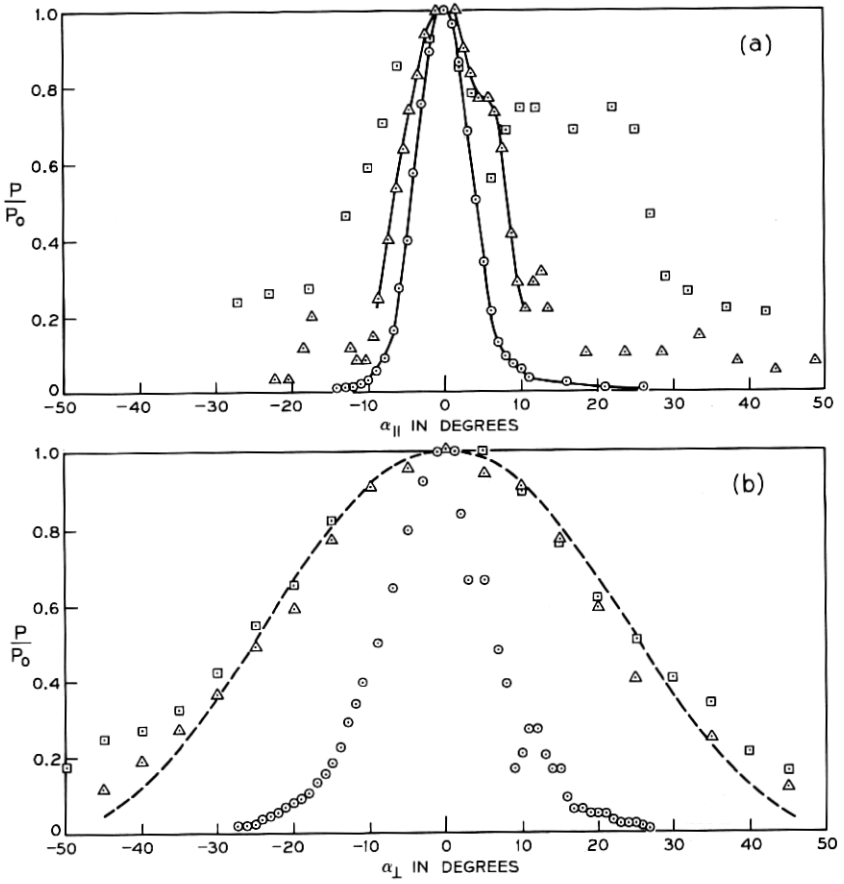

Fig. 2—Far field patterns from junction lasers. Legend: ⊙ L-229 #1, DJ laser with stripe width = 6 μm. ⊡ L-352 #2, DH laser with an oxide-masked stripe, 13 μm wide. △ L-363 #1, DH laser with a proton-bombarded stripe, 13 μm wide. (a) The lasers were rotated through an angle, $\alpha_{\parallel}$, in the plane parallel to the junction. (b) The lasers were rotated through an angle, $\alpha_{\perp}$, in the plane perpendicular to the junction. The dashed curve is a Gaussian distribution fitted to △ data.

peaks implying a multimode field distribution along the laser's junction plane. There is also more fluorescent light within the oxide-masked stripe than within the proton-bombarded stripe as evidenced by the fact that the curve described by ⊡ data points does not fall to zero (20 percent of the peak laser power propagates at large angles from the center of the junction plane).

The far field patterns perpendicular to the junction plane (Fig. 2b) are approximately Gaussian shaped for the oxide-masked and proton-bombarded DH lasers. (The dashed curve in Fig. 2b is a Gaussian distribution fitted to △ data points.) However, on the DJ profile there is evidence of a secondary lobe on the n-side of the junction plane.[2]

The width, between $1/e$ points, of far field profiles like those in Fig. 2 was used to calculate the beam dimensions on the laser mirror in directions parallel and perpendicular to the junction plane through Fig. 9 or equation (8) in Section IV. The broader profiles for DH lasers, in comparison to DJ types, illustrate their larger confinement perpendicular to the junction plane.

Sample near field measurements are contained in Fig. 3 which illustrate the normalized power distribution parallel and perpendicular to the junction plane of a DJ laser and also the profile perpendicular to the junction plane of a DH laser. The larger confinement of the DH

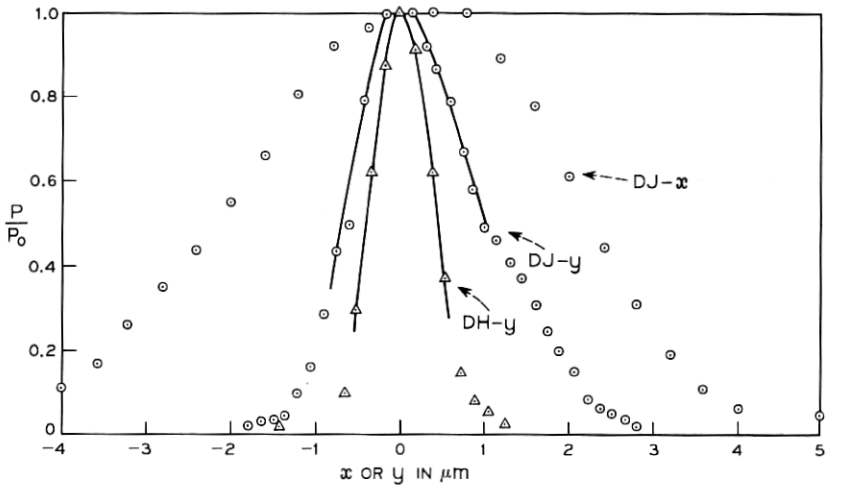

Fig. 3—Near field power distributions on the surface of junction lasers. Legend: ⊙ L-229 #1, DJ laser with stripe width = 6 μm. △ L-363 #1, DH laser with stripe width = 13 μm. Normalized power, P/P_o, is plotted versus distance, x, along the junction and distance, y, perpendicular to the junction.

laser perpendicular to the junction plane is illustrated by the curve following △ data points which is much narrower than the curves following ⊙ data points.

2.2 *Power Coupling Into Fibers*

At one end of a fiber the light emanating from the rectangular aperture on a laser was coupled into the circular core (diameter d) of a fiber across a small air gap separating the laser from the fiber. The coupling technique is diagramed in Fig. 4a for a beam which diverges at angle α_y perpendicular to the junction plane.

Power coupling measurements were made for two kinds of single-mode fibers with very different parameters. The 3.7-μm-diameter fiber, fabricated by Corning Glass Works, had a relatively low transmission loss (20 dB/km). Its characteristic number at 9000 Å is $V = 1.55$ based on Corning specifications. This information plus an estimate of the core refractive index enabled us to estimate the fiber's acceptance angle, $\theta = 7$ degrees, as well as the radius, a, to the $1/e$ point of the propagating electric field within the fiber. This is discussed further in Section IV where we find $a = 4.6$ μm. The 3.2-μm-diameter glass fiber was fabricated by DeBell and Richardson. Its parameters[3] are transmission loss ≈ 2 dB/m, $n_1 = 1.61$, $V = 2.4$ at 9000 Å, and $\theta = 12$ degrees. In Section IV we estimate $a = 2.6$ μm for this fiber. In this section we will also be describing measurements made with 10-μm and 20-μm multimode fibers ($\theta = 12$ degrees) fabricated by DeBell and Richardson.

The input tip of a fiber was cut with a razor but was not polished. It was supported on a small copper block and was held in place with epoxy. The input tip extended 20 mils over the edge of the block. The copper blocks supporting laser and fiber were mounted on separate three-dimensional micromanipulators. The output end of the fiber was immersed in oil to eliminate light reflections and light power traveling in the cladding was scattered out by immersing several inches of the fiber in oil matched to the index of the cladding. Light power leaving the output end of a fiber was maximized by adjusting the relative axial and transverse position between the fiber core and the active stripe on the GaAs chip. The micromanipulator holding the fiber had a positioning resolution of 0.125 μm. Provision was also made for reducing the tilt angles between the axes of the laser stripe and the axis of the fiber. Figure 4b contains a photograph of a permanent laser-to-fiber coupler. The picture, taken through a microscope, illustrates the 0.5-mil air gap between the surface of a DJ laser and the input tip of a 10-μm fiber. The power coupling efficiency for this coupler

was 67 percent. It did not change when the coupler was made permanent by applying epoxy between the block supporting the fiber and the block supporting the laser.

Light power from the end of a fiber was measured along with the light power radiating from the exposed laser mirror face. The detectors

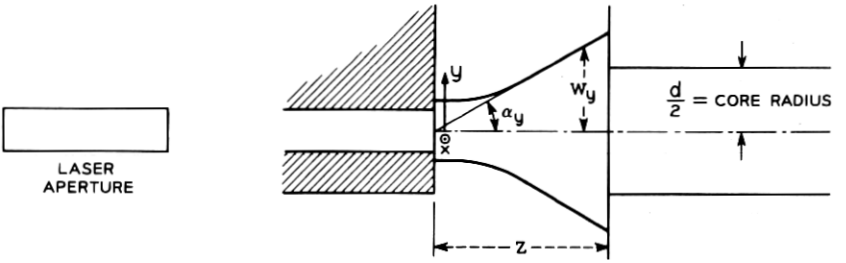

(a)

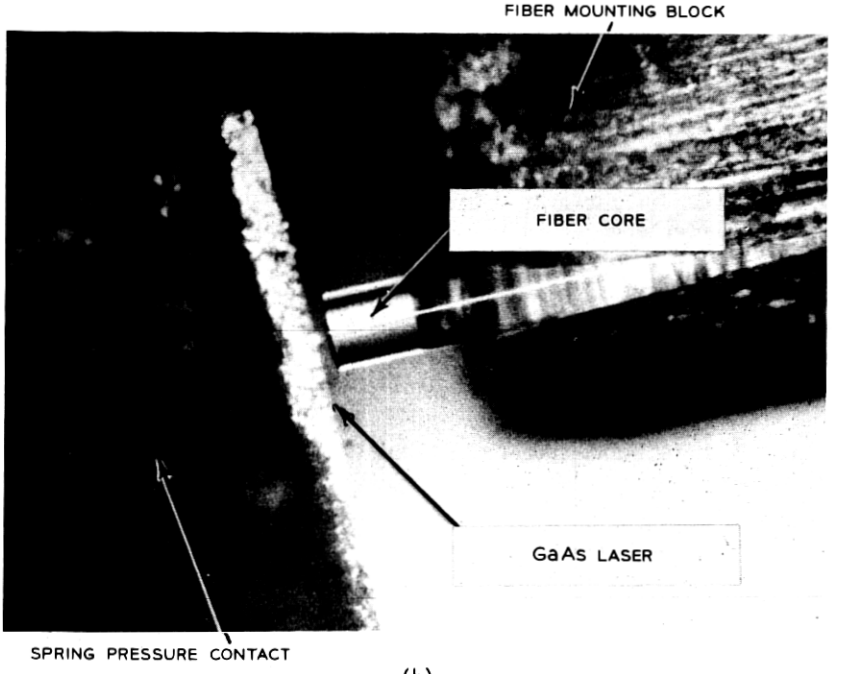

(b)

Fig. 4—(a) The Gaussian light beam emanating from a laser aperture (typical dimensions: 1 μm $\times$ 13 μm) is injected into the core of an optical fiber. In its far field the beam diverges at an angle, α_y, perpendicular to the junction plane. (b) Photograph taken through a microscope shows the 0.5-mil air gap across which light is coupled from a GaAs laser into the core of a 10-micron fiber.

used were Schottky barrier silicon photodiodes, each having an 8-nanosecond rise time, a sensitivity of 4 μA/μW at 9000 Å, and a sensitive area equal to 0.99 cm^2. Their outputs of peak power were simultaneously displayed on a dual-channel sampling oscilloscope.

The power coupling coefficient will be diminished if the axis of the laser beam is displaced from the fiber axis. This effect was measured by offsetting the fiber axis, from its optimum position, parallel and perpendicular to the junction plane. Sample results are illustrated in Fig. 5a where the fiber output power, normalized with respect to its maximum value, is plotted versus displacement along the junction plane, normalized with respect to the fiber radius. Data points ⊙, ⊗, and ◇ apply to DJ lasers. Data points △ were obtained with a DH laser (proton-bombarded stripe). The axial offset between laser and fiber was 0.5 mil for the 10-μm fiber and was less than 0.25 mil for the 3.2-μm and 3.7-μm fibers. The profile shapes are similar. For a displacement equal to one fiber radius the 10-μm fiber's output power drops to 50 percent of its optimum value. The profiles for the 3.2-μm and 3.7-μm fibers are wider between $1/e$ points possibly because mode energy extends further into the cladding. Similar measurements were made in the plane perpendicular to the junction plane of the lasers. In that plane the profiles for 3.2 μm and 3.7 μm were broader than their counterparts in Fig. 5a) reflecting the larger divergence angle perpendicular to the junction. They are not included in Fig. 5 since normalized power decreases more rapidly for offsets along the junction plane.

The effect of axially separating fibers from junction lasers is illustrated in Fig. 5b in which P/P_o is plotted versus z. Data points ◇ and △ apply to the single-mode fibers. The dashed curves are theoretical estimates based on equation (9) which is discussed in Section IV, and was derived in Ref. 4 for coupled Gaussian beams. The deviation of the ◇ data points, from the theoretical dashed curve, for large z could have resulted because of deviations of the laser beam profile from a Gaussian distribution or because the field energy propagating within the 3.7-μm fiber extended far enough into the cladding to invalidate a Gaussian approximation for the mode profile. The 10-μm and 20-μm multimode fibers (data points ⊗ and ○) begin to lose light when they are axially separated by more than a critical distance, $Z_c \approx (d/2)/\tan\theta$, at which some rays of laser light within the fiber's acceptance cone do not intercept the fiber's core. The critical distance for fibers with a $\theta = 12$ degrees acceptance angle is 24 μm (experimental distance $\approx$ 19 μm) for 10-μm-diameter fibers and 46 μm (experimental

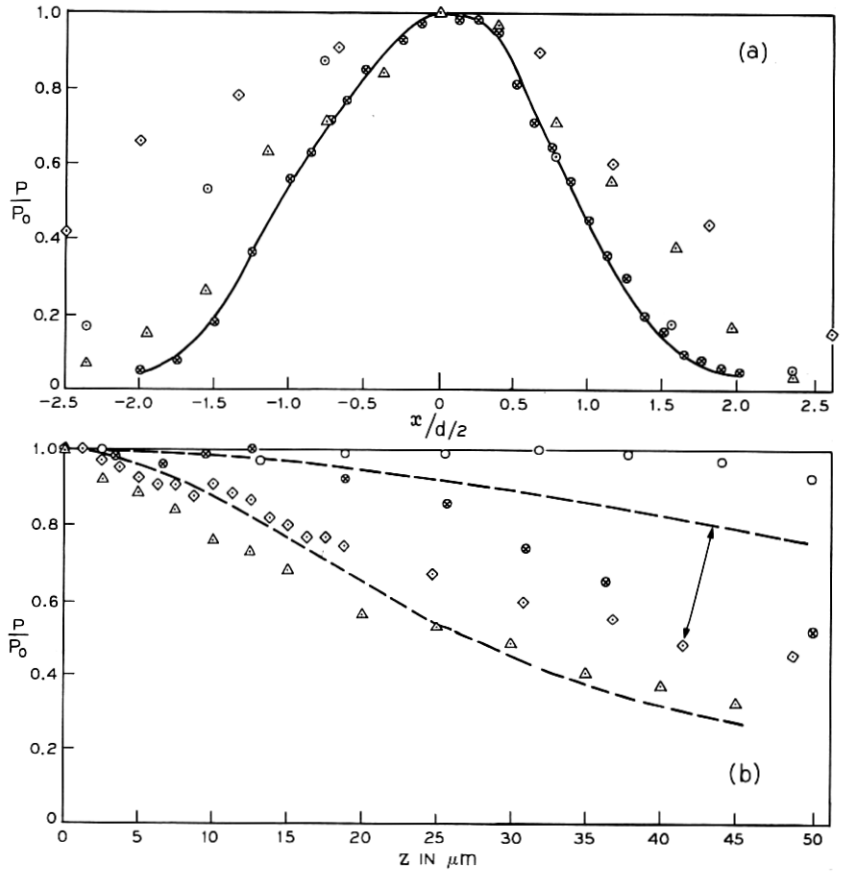

Fig. 5—Profiles of the normalized power emitted from the end of a fiber which was displaced from its optimal position relative to the laser stripe.

Legend: ⊙ 3.2-μm fiber
⊗ 10-μm fiber } L-229 #1 DJ laser
○ 19-μm fiber
◇ 3.7-μm fiber, L-229 #2 DJ laser
△ 3.2-μm fiber, L-363 #1 DH laser.

(a) The fiber core was offset in the plane of the junction. (b) The fiber core was axially separated from the laser surface. The dashed curves were based on equation (9) with $\lambda = 9000$ Å. ($w_{o_x} = 2.7$ μm, $w_{o_y} = 1.3$ μm, $a = 4.6$ μm for ◇ data; $w_{o_x} = 1.5$ μm, $w_{o_y} = 0.36$ μm, $a = 2.6$ for △ data.)

distance $\approx$ 45 μm) for 20-μm fibers. Agreement with experiment is very good for the multimode fibers.

Table I is a summary of experiments performed with two lasers from a diffused junction batch (L-229, stripe width = 6 μm), two lasers from a double-heterostructure batch with proton-bombarded stripes (L-363, stripe width = 13 μm), and two lasers from a DH batch with oxide-masked stripes (L-352, stripe width = 13 μm). Measured power coupling coefficients, κ, are listed for a variety of fibers. The fiber parameters, listed in Table II, are core diameter, d; percent index mismatch between core and cladding, Δ; acceptance angle, θ; characteristic number, V; and number of propagating modes, N. The laser parameters are threshold current, I_{th} ; far field divergence angles, α_x and α_y ; and the beam half-widths, w_{ox} and w_{oy} , at the surface of the laser. Parameters w_{ox} and w_{oy} were determined in two ways: directly ($w_{ox\ exp}$, $w_{oy\ exp}$) from near field measurements or by extrapolating ($w_{ox\ theor}$, $w_{oy\ theor}$) from measurements of the far field divergence angles α_x , α_y by using Fig. 9 or equation (8) in Section IV. The mode dimension $w_{ox\ theor}$ for DH laser L-352 #1 was extrapolated from the width between $1/e$ points of the larger of the two peaks on the multimode far field profile in Fig. 2a. The $1/e$ points were measured relative to the fluorescent light level, $P/P_o = 0.2$. For every laser $w_{oexp} > w_{otheor}$ which implies a greater beam expansion than can be theoretically accounted for by a Gaussian beam having its waist located on the end surface of the laser. The discrepancy implies that the beam waist is located several microns from the end of the lasing stripe. An estimate of the location of the beam waist within the laser cavity is derived from the Gaussian beam expansion curves discussed in Section IV and plotted in Fig. 10a using the beam waist radius, w_o , as the parameter. For DH lasers, the beam waist parallel to the junction plane is located inside the laser around 8 μm from the laser mirror; perpendicular to the junction plane the beam waist is located also inside the laser, about 7 μm from the mirror. For DJ lasers, the beam waist perpendicular to the junction plane is approximately on the laser mirror; parallel to the junction plane, the beam waist is about 8 μm from the mirror.

Theoretical estimates of the power coupling coefficient, κ, based on the laser and fiber parameters, were computed from equation (9) for a Gaussian laser beam. They are listed in Table I for comparison with the measurements. The far field pattern (Fig. 2a) for DH laser L-352 #1 implies a multimode field distribution along its junction plane. The theoretical estimate of κ for DH laser L-352 #1 assumes that 67

TABLE I—SUMMARY OF MEASUREMENTS FOR DIFFUSED JUNCTION LASER (DJ) AND DOUBLE-HETEROSTRUCTURE LASERS (DH) WITH PROTON-BOMBARDED (DH-P) OR OXIDE-MASKED STRIPES (DH-O)

	Laser Parameters							κ							
#	I_{th} (amps)	α_x (deg)	α_y (deg)	w_{0_x} theor. (μm)	w_{0_x} exp. (μm)	w_{0_y} theor. (μm)	w_{0_y} exp. (μm)	Fiber 1 theor. (%)	Fiber 1 exp. (%)	Fiber 2 theor. (%)	Fiber 2 exp. (%)	Fiber 3 theor. (%)	Fiber 3 exp. (%)	Fiber 4 theor. (%)	Fiber 4 exp. (%)
DJ															
L-229 #1	5.6	5	10	2.3	3.6	1.2	1.4		—	72	48	86	73	86	75
#2	7	4.3	8.9	2.7	3.2	1.3	1.5	37	26	77	42	88	64	88	67
DH-P															
L-363 #1	0.59	7.5	29	1.5	2.1	0.36	0.65	8.7	4.6	23	25	38	29		
#2	0.48	12	27	0.95	—	0.40	—		—	18	13	35	24		
DH-O															
L-352 #1	0.73	9.3	26	1.3	1.6	0.43	0.73	8.8	4.3	22	14	40	26		
#2	0.83	13	32	0.88	—	0.33	—	3.5	2.5	9.8	6.5	20	18		

TABLE II—FIBER PARAMETERS (λ = 9000 Å)

#	d (μm)	Δ (%)	θ (deg)	V*	N
1	3.7	0.36	7.1	1.6	1
2	3.2	0.82	12	2.3	1
3	10	↓	↓	7.2	15
4	19			14	98

* $V < 2.41$ for single-mode fibers

percent of the beam power is contained within the dominant Gaussian mode of the laser. The calculation of κ_{theor}, in Table I, assumes that the beam waist is located on the laser mirror. The error caused because the beam waist may actually be located 8 μm from the end of the stripe is derived from Fig. 11 [plotted from equation (9)] which contains curves of κ versus z, with w_o as the parameter, for 3.2-μm and 3.7-μm single-mode fibers. The coefficient, κ, is reduced by 5 percent when a $w_{o_y} = 0.5$ μm beam is separated by 7 μm from a 3.2-μm fiber. The reduction is 3 percent when a $w_{o_x} = 1.5$ μm beam is separated by 8 μm from a 3.2-μm fiber. Therefore, the theoretically expected values of κ for 3.2-μm fibers listed in Table I may be too high by as much as 8 percent because the actual beam waist occurs inside the lasing cavity. Similar arguments, applied to 3.7-μm fibers, indicate that K_{theor} may be too high by 3 percent.

The measured values of κ, listed in Table I, were obtained by extrapolating* the lasing light power emitted from a 30-cm length of fiber back to its input tip and comparing it with the total lasing power radiating from the active stripe on the GaAs chip. Power radiating from the stripe is fluorescence until the pump current exceeds the laser's threshold current. Fluorescent light was identified from measurements of total radiated power versus pump current. Figure 6 contains measurements for two DH lasers, one with a proton-bombarded stripe (data points: $\triangle$) and the other with an oxide-masked stripe (data points: $\square$) in which fluorescent light is more prevalent. In the curve for the oxide-masked stripe, fluorescent power is 46 percent of the total laser power when the pump current is 10 percent above threshold.

* The 3.7-μm fiber had a relatively low transmission loss (20 dB/km). Therefore, the power at an input tip is almost equal to the power leaving the output end of a 30-cm length. The transmission loss for DeBell and Richardson fibers is approximately 2 dB/m at 9000 Å. Thus the power at an input tip is about 1.2 times greater than the power emanating from the output end of a 30-cm length.

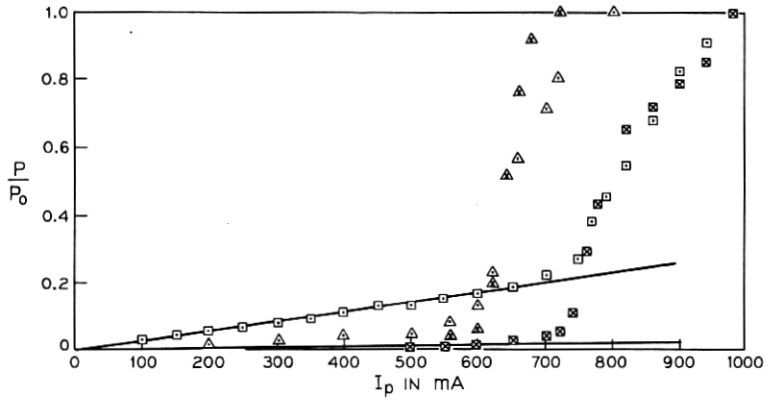

Fig. 6—Normalized power radiated from the laser surface versus pump current: ⊡ L-352 #1, DH laser with oxide-masked stripe; △ L-363 #1, DH laser with proton-bombarded stripe. Normalized power leaving the end of a 3.2-μm fiber versus pump current: ⊠ L-352 #1, DH laser; ▲ L-363 #1, DH laser.

The coupling coefficient with fluorescent light included is 56 percent of its value when the fluorescent component is subtracted away from the total power radiating from the laser.

The coupling coefficients (fluorescent power not included), listed in Table I, were measured for pump currents about 10 percent above threshold within the laser's linear operating region. In general the measured power coupling coefficients in Table I are in good agreement with theory. The cases where the discrepancy is large may have arisen because of deviations of the beam profile from a Gaussian shape or because the field energy propagating within the single-mode fibers penetrated far enough into the cladding to invalidate a Gaussian approximation for the mode profile. The relatively small theoretical coupling coefficients listed in Table I occur because the beam half-width at its waist, $w_{o_{y\ \mathrm{theor}}}$, is considerably smaller than the radius, a, of the propagating mode in the 3.7-μm (a = 4.6 μm) and 3.2-μm (a = 2.6 μm) fibers. In Section III we propose to increase κ by using a cylindrical lens attached to the input tip of a fiber.

III. LENS DESIGN FOR BEAM COLLIMATION

The Gaussian beam emanating from the rectangular aperture on a GaAs injection laser diverges much more rapidly perpendicular to the junction plane than it does parallel to the junction plane. A cylindrical lens can be designed to collimate the laser beam perpendicular to the junction plane and in that way eliminate decoupling due to the

mismatch between the curved wavefront of the propagating mode in a single-mode fiber. Furthermore, the beam cross section can be made square instead of rectangular if the lens is designed to collimate when the beam width perpendicular to the junction is equal to the beam width along the junction. Then, if needed, two spherical lenses can be used to focus the beam into a circular fiber of arbitrary diameter.

Figure 7a illustrates one arrangement with the lens in contact with the fiber core. The parameters to be calculated are the radius of curvature of the lens and its axial offset from the surface of the laser.

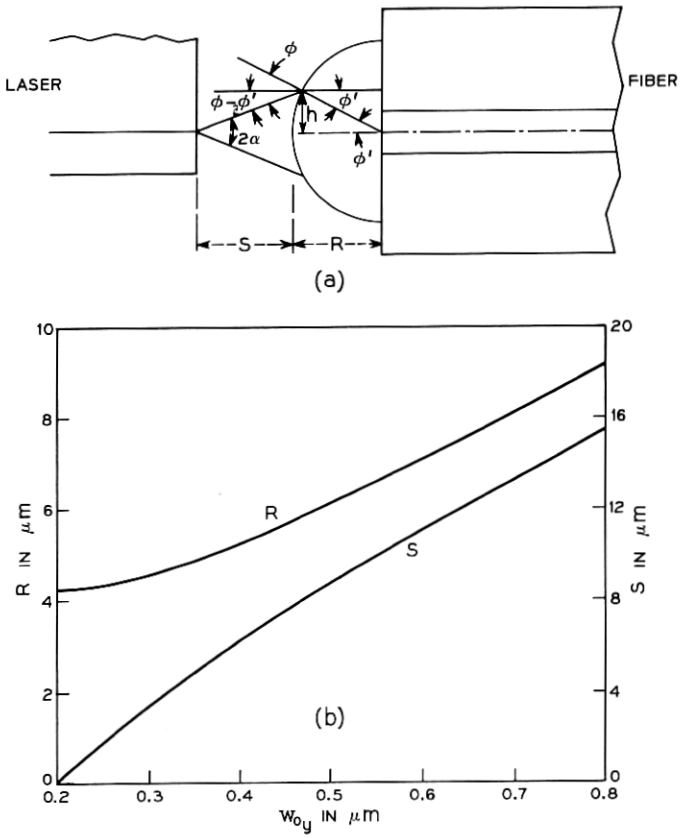

Fig. 7—(a) Cylindrical lens arrangement for collimating the laser beam perpendicular to the junction plane. (b) The radius of curvature, R, of a cylindrical lens and its axial offset, s, from the surface of a laser are plotted versus w_{0y}, the mode width perpendicular to the junction plane. The lens is designed to collimate the beam (λ = 9000 Å) to a 6-μm half-width perpendicular to the junction plane.

These parameters are functions of the divergence angle, α, of the laser beam; the height at which the beam is to be collimated, h; and the refractive index, n', of the lens glass. Using Fig. 7a as a reference we may write down a system of equations to determine the lens parameters.

The angle of refraction, ϕ', within the lens is defined by:

$$\sin \phi' = \frac{h}{R}. \tag{1}$$

From Snell's Law, ϕ' may be written in terms of the angle of incidence, ϕ,

$$\frac{\sin \phi}{\sin \phi'} \approx \frac{\phi}{\phi'} = n'. \tag{2}$$

The divergence angle, α, of the laser beam may be related to ϕ and ϕ' through

$$\alpha = \phi - \phi'. \tag{3}$$

The offset distance, s, from the surface of the laser may be determined by applying the law of sines:

$$s = R\left(\frac{\sin \phi}{\sin \alpha} - 1\right). \tag{4}$$

In the following we assume that the refractive index of the glass is $n' = 1.5$ and that the Gaussian light mode fills a 12-μm-wide stripe along the junction ($w_{o_x} = 6$ μm, $h = w_{o_x}/\sqrt{2} = 4.2$ μm). The lens parameters, R and s, may easily be recomputed for different mode widths, w_{o_x}, because they are linearly related. Equations (1) through (4) (with $\lambda = 9000$ Å) were used in Fig. 7b to plot R and s as a function of $w_{o_y} = \lambda/(\sqrt{2}\,\pi \tan \alpha)$, the radius of the beam waist perpendicular to the junction. The smallest beam waist (maximum divergence angle) which can be collimated to 12 μm is $w_{o_y} = 0.2$ μm ($\alpha_y = 45$ degrees). As a practical example, consider $w_{o_y} = 0.5$ μm ($\alpha_y = 22$ degrees) for which $R = 6.1$ μm, $s = 8.7$ μm.

One technique for fabricating the cylindrical lens might involve grinding an unclad cylindrical fiber in half.[5] To perform this operation[6] we have constructed a heavy brass lap as illustrated in Fig. 8. The top surface of the lap was surface-ground and 90-degree v-grooves, 2 mils deep, were scribed across it. The procedure involves laying unclad fibers on the bottom of the grooves and holding them in place with wax that can be dissolved by acetone. The grinding is done by turning the brass lap over and polishing its surface down against a wet slurry containing 1-μm carborundum particles.

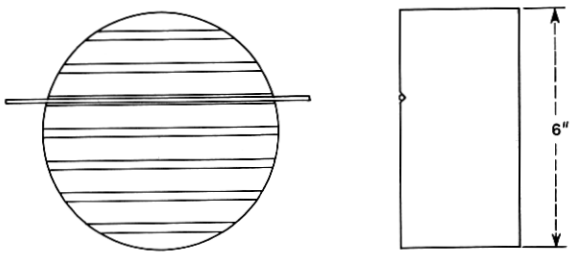

Fig. 8—Brass lap for grinding the surface of an unclad cylindrical fiber.

In a properly fabricated laser-lens-fiber system the sole cause for power decoupling should be due to the mismatch in size between a 6-μm $\times$ 6-μm laser beam and a field of radius, a, propagating within a single-mode fiber. From equation (9) (with $z = 0$) in Section IV we have $\kappa = 2/(6/a + a/6)^2$. If the DeBell and Richardson fiber ($a = 2.6$ μm) is used then $\kappa = 51$ percent* is a lower bound on κ for $1.1 < w_{o_x} < 6$ μm. If the 3.7-μm Corning fiber ($a = 4.6$ μm) is used then $\kappa = 90$ percent* is a lower bound for $3.6 < w_{o_x} < 6$ μm.

IV. COMPUTATION OF POWER COUPLING COEFFICIENTS

The dominant transverse mode of an injection laser has an astigmatic Gaussian spatial distribution. When this mode is injected into an optical fiber a set of modes of the fiber is excited. If the fiber is multimode then it can accept all power within the laser Gaussian distribution that radiates within a cone angle which is less than the fiber's acceptance angle. If the fiber is single-mode then it can only support the HE_{11} mode which we will approximate by a Gaussian distribution. An existing theory[4] for coupling power between two Gaussian beams will be used to compute the power coupling coefficient for injection lasers feeding single-mode fibers.

4.1 *Power Coupling Into a Single-Mode Fiber*

In the following we assume that a Gaussian field $\epsilon(x, y, z)$ emanates from a rectangular aperture on a cleaved GaAs chip (refer to Fig. 4a) and propagates in space along direction z:

$$\epsilon = E(z) \exp\left\{-\left[\left\{\left(\frac{x}{w_x}\right)^2 + \left(\frac{y}{w_y}\right)^2\right\} + j\frac{K}{2}\left\{\frac{x^2}{R_x} + \frac{y^2}{R_y}\right\}\right]\right\}. \quad (5)$$

* These estimates include a 4-percent reflection loss at the input surface of the lens. If the lens surface is made reflectionless then $\kappa = 53$ percent is a lower bound for the 3.2-μm fiber and $\kappa = 94$ percent is a lower bound for the 3.7-μm fiber.

The beam parameters at a convenient reference plane separated by distance, z, from the laser surface are the beam radii w_x , w_y parallel and perpendicular to the laser's junction plane and the wavefront radii of curvature R_x , R_y parallel and perpendicular to the junction plane. For a one-dimensional beam, parameters w and R, at the reference plane, may be written in terms of their values ($w = w_o$, $R_o = \infty$) at the surface of the laser, $z = 0$.[4]

$$w^2 = w_o^2\left(1 + \frac{z^2}{w_o^2}\tan^2\alpha\right), \tag{6}$$

$$\frac{1}{R} = \frac{2\,\frac{z}{w_o^2}\tan^2\alpha}{\left(1 + 2\,\frac{z^2}{w_o^2}\tan^2\alpha\right)}, \tag{7}$$

where

$$\tan\alpha = \frac{\lambda}{\sqrt{2}\,\pi w_o}. \tag{8}$$

In its far field, the width to the $1/e$ point of a Gaussian beam power distribution diverges at angle α. Figure 9, based on equation (8) with $\lambda = 9000$ Å, illustrates a graph of α versus w_o , the half-width of the electric field at the beam waist. Figure 10 contains plots of w and R versus z with w_o , as the parameter, and $\lambda = 9000$ Å. The beam width is collimated in its near field. The wavefront leaves the laser aperture as a plane wave but begins to curve as the beam width begins to enlarge.

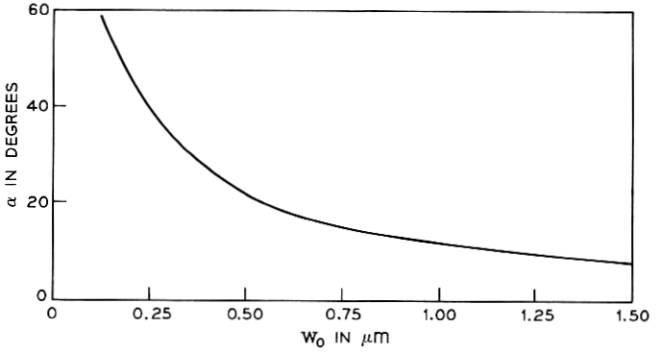

Fig. 9—The far field divergence angle, α, of a Gaussian power distribution is plotted versus the half-width, w_o, of the electric field at the beam waist ($\lambda = 9000$ Å). $\alpha = \tan^{-1}\lambda/\sqrt{2}\,\pi w_0$.

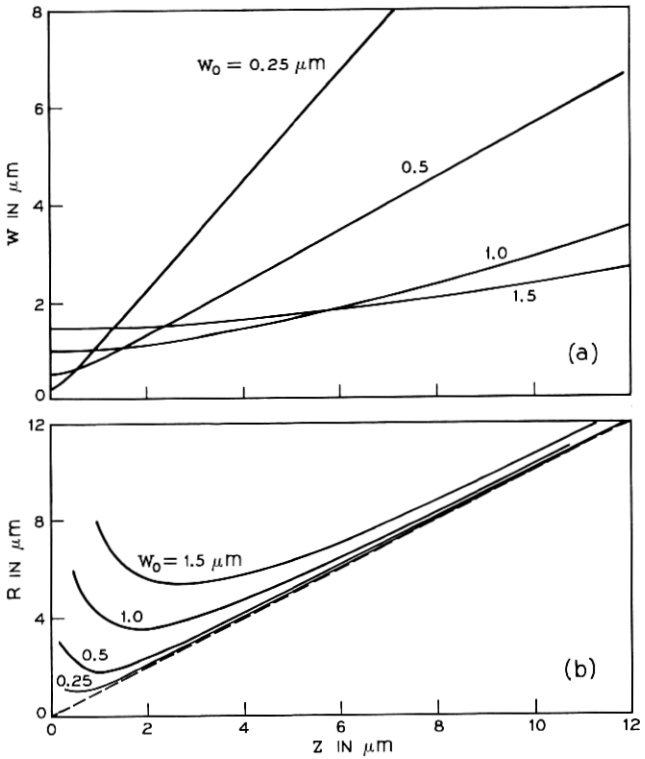

Fig. 10—(a) The half-width, w, of a Gaussian beam is plotted versus z, the separation of the reference plane from the plane of the beam waist (λ = 9000 Å). The half-width, w_o, of the electric field at z = 0 is the parameter. (b) The wavefront radius of curvature, R, is plotted versus z (λ = 9000 Å). w_o is the parameter.

In the far field of the beam both w and R expand linearly with Z. The width of the beam, $2w_o$, at the laser surface may be deduced from equation (8) and far field measurements of α as described in Section 2.1. Sample results are listed under the columns marked α and $w_{o\text{theor}}$ in Table I. The near field measurements discussed in Section 2.1 illustrate how to measure w_o directly. Sample measurements are listed in the column marked $w_{o\text{exp}}$.

For lasers with rectangular symmetry, the expression for the percent power, κ, coupled from a Gaussian laser beam represented by parameters w_{ox}, w_{oy} into another Gaussian distributed field (for the fiber mode) represented by parameters $R = \infty$, $w = a$ is:[4]

$$\kappa = \frac{\left(\frac{w_{ox}}{a} + \frac{a}{w_{ox}}\right)^2}{\sqrt{1 + \frac{2z}{K(w_{ox}^2 + a^2)}}} \frac{\left(\frac{w_{oy}}{a} + \frac{a}{w_{oy}}\right)^2}{\sqrt{1 + \frac{2z}{K(w_{oy}^2 + a^2)}}} \tag{9}$$

where $K = (2\pi)/\lambda$ is the propagation constant in free space.

The parameter, a, is the mode radius within a single-mode fiber. It can be estimated from knowledge of the characteristic number, V, of the fiber waveguide which was $V = 2.3$ ($\lambda = 9000$ Å) for the 3.2-μm DeBell and Richardson fiber and was $V = 1.6$ ($\lambda = 9000$ Å) for the 3.7-μm Corning fiber. Since $V < 2.4$ for both fibers, the HE_{11} mode is the only one guided and the percent power in the core may be estimated from the curves of P_{core}/P_{clad} versus V in Ref. 7. For the 3.2-μm fiber 79 percent of the power travels within the core but for the 3.7-μm fiber only 57 percent of the power travels within the core. If the HE_{11} mode is approximated by a Gaussian distribution then the radius, a, of the $1/e$ point of the field intensity can be determined from knowledge of $P_{core}/(P_{core} + P_{cladding})$. We find that $a = 2.6$ μm for the 3.2-μm fiber and $a = 4.6$ μm for the 3.7-μm fiber.

The one-dimensional form of equation (9) was used in Fig. 11a to plot κ (parallel or perpendicular to the junction plane) versus axial separation, z, between either the 3.2-μm fiber ($a = 2.6$ μm, solid curves) or the 3.7-μm fiber ($a = 4.6$ μm, dashed curves) and lasers parametrized by w_o (the radius of the beam waist parallel or perpendicular to the junction plane). The coefficient, κ, sloughs off gradually in the laser's far field due to the increasing mismatch between the beam and mode diameters. The phase mismatch between the curved laser beam wavefront and the planar mode has a marked influence on κ in the near field region where the radius of the wavefront is in the vicinity of its minimum value.

4.2 *Power Coupling Into Multimode Fibers*

The core of a fiber waveguide can accept those rays of laser light which diverge from the lasing slit at angles equal to or less than the acceptance angle, θ, of the fiber where

$$\begin{aligned} \theta &= \sin^{-1}(n_1^2 - n_2^2)^{\frac{1}{2}}, \\ n_1 &= \text{refractive index of core}, \\ n_2 &= \text{refractive index of cladding}. \end{aligned} \tag{10}$$

Assume that the laser beam is Gaussian-distributed along x and y

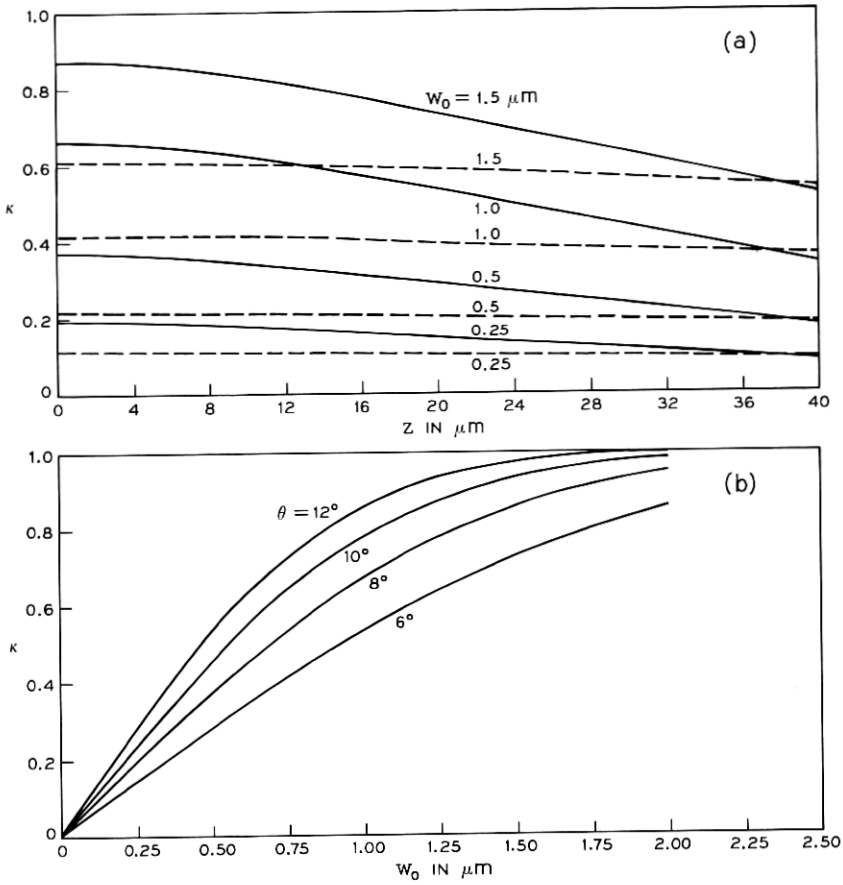

Fig. 11—(a) Power coupling coefficient, κ, is plotted versus axial separation, z, between a laser and a single-mode fiber (λ = 9000 Å). The half-width, w_o, of the laser beam waist is the parameter. Solid curves apply to a 3.2-μm fiber (mode radius = 2.6 μm). Dashed curves apply to a 3.7-μm fiber (mode radius = 4.6 μm). (b) κ is plotted versus w_o (λ = 9000 Å). Fiber acceptance angle, θ, is the parameter.

and that the beam remains collimated along the junction plane. In its far field perpendicular to the junction, the beam half-width increases linearly,

$$w = \sqrt{2}\, z \tan \alpha. \tag{11}$$

The Gaussian power distribution may be expressed as follows:

$$P \propto e^{-2y^2/w^2}. \tag{12}$$

We now compute the fraction of the laser power which travels within

a cone angle equal to θ, the acceptance angle of the fiber. The area subtended by this cone on the fiber end has a half-width, θz. Therefore, the power coupling coefficient, κ, into a multimode fiber with acceptance angle, θ, is:

$$\kappa = \frac{\int_0^{\theta z} e^{-2y^2/w^2}\, dy}{\int_0^{\infty} e^{-2y^2/w^2}\, dy} = \frac{\int_0^{2\pi w_o \theta/\lambda} e^{-t^2/2}\, dt}{\int_0^{\infty} e^{-t^2/2}\, dt} \tag{13}$$

where:

$$t = \frac{2y}{w} = \frac{2\pi w_o y}{\lambda z}. \tag{14}$$

The coefficient, κ, is plotted versus w_o (the half-width of the electric field on the laser mirror) in Fig. 11b. Fiber acceptance angle, θ, is the parameter and λ = 9000 Å.

V. CONCLUSIONS

Experiments have been performed with diffused junction lasers and with double-heterostructure lasers whose stripes were formed by proton bombardment or oxide masking. The far field radiation patterns of DH lasers were considerably broader perpendicular to the junction reflecting their larger confinement in that plane. The patterns along the junctions of DJ lasers were more Gaussian-like than those for DH lasers. Fluorescent light was more prevalent and higher-order modes were more evident with oxide-masked stripes than for those with proton-bombarded stripes.

Theoretical estimates have been calculated for κ, the efficiency for coupling light power from junction lasers into single- and multimode fibers. The highest measured values for κ were:

(*i*) 73 percent (theoretical estimate = 86 percent) for coupling power from DJ lasers into 10-μm fibers.

(*ii*) 48 percent (theoretical estimate = 72 percent) for coupling power from DJ lasers into 3.2-μm single-mode fibers and 26 percent (theoretical estimate = 37 percent) for coupling power from DJ lasers into 3.7-μm single-mode fibers.

(*iii*) 25 percent (theoretical estimate = 23 percent) for coupling power from a DH laser, with a proton-bombarded stripe, into a 3.2-μm single-mode fiber and 5 percent (theoretical estimate = 9 percent) for coupling into a 3.7-μm single-mode fiber.

From theory, the major causes for reduced power coupling between two well-aligned Gaussian beams is a mismatch between the beam diameters at their waists or else a mismatch between the shapes of their wavefronts if the beam waists are axially separated from one another. Our measurements in the near field of DH and DJ laser beams[2] imply a larger beam expansion than can be theoretically accounted for by a Gaussian beam having its waist located on the end surface of the laser. In Section 2.2 we showed that the reduction in the expected value of κ is small (less than 8 percent) if the laser beam waist is located, within the lasing cavity, approximately 8 μm from the end of the stripe. The primary reason for relatively small coupling into the single-mode fibers we measured is the mismatch in diameter of the laser beam waist perpendicular to the junction from the larger diameter field propagating within the fiber. A cylindrical lens has been designed to increase κ by:

(*i*) Allowing the beam radius to increase perpendicular to the junction and then collimating it when it more closely matches the diameter of the propagating mode within the fiber (the beam is essentially collimated along the junction).

(*ii*) Transforming the beam's rectangular cross section into a square so that a spherical lens can be used to further match the beam diameter to the field diameter within the fiber.

The lens design curves indicate the need for a 6-μm radius of curvature. We are attempting to fabricate lenses by grinding cylindrical fibers in half.

VI. ACKNOWLEDGMENTS

The author gratefully acknowledges the helpful suggestions of T. P. Lee and J. C. Dyment.

REFERENCES

1. Dyment, J. C., D'Asaro, L. A., North, J. C., Miller, B. I., and Ripper, J. E., "Proton Bombardment Formation of Stripe Geometry Heterostructure Lasers for 300°K C. W. Operation," to be submitted for publication in Proc. IEEE.
2. Zachos, T. H., and Dyment, J. C., "Resonant Modes of GaAs Junction Lasers—III: Propagation Characteristics of Laser Beams with Rectangular Symmetry," IEEE J. Quant. Elect., *QE-6*, (June 1970), pp. 317–324.
3. Tynes, A. R., Pearson, A. D., and Bisbee, D. L., "Loss Mechanisms and Measurements in Clad Glass Fibers and Bulk Glass," J. Opt. Soc. Amer., *61*, No. 2 (February 1971), pp. 143–153.
4. Kogelnik, H., "Coupling and Conversion Coefficients for Optical Modes," in *Proceedings of the Symposium on Quasi-Optics*, edited by J. Fox (Polytechnic Press, Brooklyn, 1964).
5. Marcatili, E. A. J., private communication.
6. Glynn, P., private communication.
7. Gloge, D., unpublished work.